Type of contribution:

- Editorial
- ▶ Research Paper
- Case Study
- Review Paper
- Scientific Data
- Report of Tech. Application

Mechanical Engineering for Society and Industry
Vol. 4, No. 1 (2024) pp 103-114
https://doi.org/10.31603/mesi.11443
e-issn. 2798-5245

Rheological modelling of carbonyl-iron particles (CIP) paraffin oil-based magneto-rheological fluids

Eyere Emagbetere, Olusegun David Samuel*, Omonigho Benedict Otanocha

Department of Mechanical Engineering, Federal University of Petroleum Resources, Effurun, P.M.B 1221, Delta State, **Nigeria**

✉ samuel.david@fupre.edu.ng

This article contributes to:

7 AFFORDABLE AND CLEAN ENERGY

SUSTAINABLE DEVELOPMENT GOALS

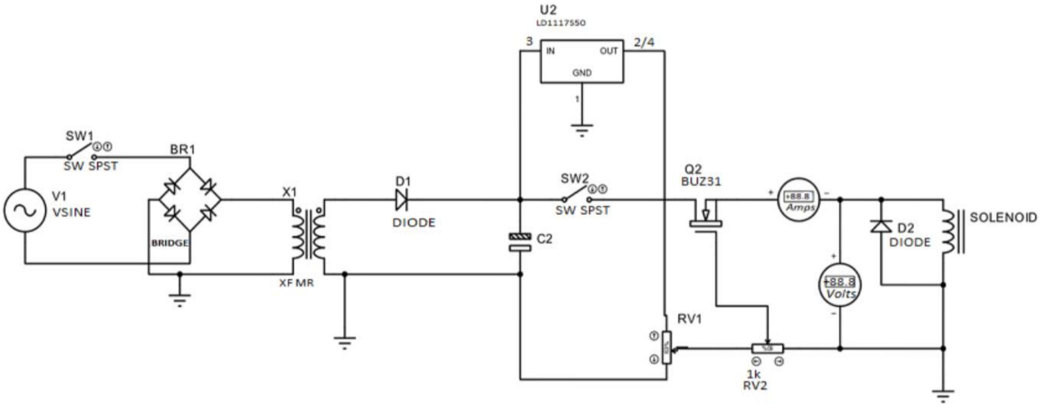

Highlights:

- Five rheological models were developed for a novel CIP paraffin oil-based MR fluid.
- A maximum viscosity of 45 Pa.s was obtained for the MRF consisting of 70% CIP and 3% grease additive by mass.
- The strengths and limitations were obtained from the comparison of numerical and experimental datasets.
- The predicted outcomes of the different models varied significantly (P-value << 0.05).
- The Bingham model achieved the highest accuracy (R^2=0.98) for predicting MR fluid viscoelastic behaviour.

Abstract

New types of magneto-rheological fluids are increasingly being developed lately, but there is a dearth of information on the performance of commonly used rheological models for emerging MRFs such as carbonyl-iron particles (CIP) paraffin-oil-based MRF. This work aims to investigate the performance of some rheological models for application in predicting shear stress and yield strength in an emerging MRF suitable for flow-mode applications. CIP, low viscosity paraffin oil, and lithium grease were used as magnetic particles, carrier fluid, and additives, respectively, to prepare the MRF. Based on different mixing proportions determined with the Taguchi method of experimental design, sixteen samples were prepared following a standard procedure. For each sample, the values of viscosity and shear stress were determined using a viscometer and rheometer, respectively, with an incorporated self-developed magnetic device. By fitting the data and using the multi-objective nonlinear programming solver in Micro-soft Excel to determine optimum parameters for each model, the Bingham Model, Herschel–Bulkley Model, Casson Model, Cross models, and Power-law were used to model the experimental data. Predicted shear stress values and yield strength were then analyzed using ANOVA at a 5% confidence level. The relative errors were determined using RMSE, Mean Square Error, and Mean Absolute Error. There was a significant variation in the predicted outcomes of all the models. Overall, all the models gave relatively acceptable results. However, the Herschel-Bulkley model gave the best results, while the Casson model gave the worst results, judging by their values of errors. It is shown that the Herschel-Bulkley model should be best used for predicting the rheological characteristics of CIP and paraffin oil-based MRF.

Keywords: Magnetic fluids; Magnetic particles; Rheological models

Article info

Submitted: 2024-05-25

Revised: 2024-07-06

Accepted: 2024-07-25

Publisher

Universitas Muhammadiyah Magelang

1. Introduction

Recently, there has been a lot of interest in magneto-rheological fluids (MRFs) due to their remarkable capacity to modify their rheological reactions to external magnetic fields [1]. A family of smart materials known as MRF is created by scattering magnetic or ferrous particles in a carrier fluid. Viscosity and flow behaviour may be controlled to an unprecedented degree through the use of an induced magnetic field, making them extremely useful in a variety of engineering applications [2]. The potential engineering applications of MRFs are extensive and have been demonstrated in various fields ranging from adaptive shock absorbers in vehicles to vibration control devices and tunable stiffness structures. Multifaceted and promising are the practical applications of MRF technology [3]. Many technologies, including dampers, gearboxes, centrifugal fans, hydraulic machines, jet stabilization, mechanical sealing, polishing, and prostheses, have made extensive use of them [4].

Ideally, MRF contains magnetic particles like magnetite, ferrite, carbonyl iron and iron oxides, which are dispersed in a carrier fluid such as silicone oil, mineral oil or water, with specific additives added to address certain problems. Preparation methods and the properties of various types, particularly magnetic composites with soft magnetic particles and polymers, are reviewed in the literature [5]. To date, efforts are geared towards developing more affordable and stable MRFs, extending their applications, and developing suitable models for their study, simulation, and control [5]. CIP paraffin-oil-based MRF is a potentially inexpensive type of MRF that can be produced from readily available materials that can be sourced locally. Various modelling approaches have been adopted for MRFs One common approach is to identify a suitable rheological model and then determine the correct model parameters for the specific MRF being studied [2]. Different variables (MRF properties) can be studied and mathematically related regardless of the modelling methodology. Some variables that are commonly studied and modeled include shear stress, shear strain, viscosity, volume ratio, type and shape, properties of carrier fluids, the introduced magnetic field capacity, particle dimensions, and style of operation. So far, various models have been reported in several review works [2], [5]. Improved design strategies are masterminded by an understanding of the rheological behaviour of CIP-Paraffin-Oil-based MRFs [6]. Outstanding rheological properties of magnetorheological fluids with various types of surfactants are documented in the literature. For instance, the rheological properties of magnetic fluids with nonpolar and polar carrier liquids [7], high- concentrations of ferrofluids [8], iron nanoparticle core–shell structures [9], and carbonyl iron/strontium hexaferrite [10] have been studied.

Table 1 highlights an overview of performance indicators of rheological properties of diverse surfactants in MRFs. Modelling of the magnetic field has been found to be rather uncomplicated compared to modelling of the fluid flow field, which is rather complicated. In all of the conducted research, different models were used to suit the conditions and properties of the synthesized fluid. None of these models can be used in all situations, and each one has its own limitations. Therefore, the establishment of a comprehensive model that can be used for predicting the rheological behaviour of different synthesized fluids at different conditions is crucial. Several studies have demonstrated the impact of magnetic field strength and orientation on viscosity and shear stress, adding a layer of complexity to the modelling process [11], [12]. These models are more suitable for the particular MRF they investigated and may not be adequate for other MRFs. Meanwhile, the industrial application of MRFs generally requires accurate rheological models to provide the necessary foundation for predicting and optimising their behaviour in response to external forces [2]. Therefore, further research is needed to develop rheological models that can effectively predict the behaviour of these fluids under different conditions to unravel complex behaviours and fully understand their dynamics for their potential real-world applications. This study delves into the intricacies of rheological modelling, focusing specifically on MRFs formulated with CIP and paraffin oil. The combination of CIP's magnetic properties and Paraffin Oil's stability would result in MRFs that exhibit unique features, including cost-effectiveness and tunable rheological behaviours [13]–[15]. Understanding and predicting the rheological characteristics of these CIP paraffin oil-based MRFs is paramount for their effective utilisation in engineering applications. In order to improve the predictive power of these models for performance optimisation in real-world scenarios, the study builds a theoretical framework using knowledge from earlier research [12], [13]. A significant aspect of this exploration involves the influence of external magnetic fields on the rheological properties of CIP Paraffin Oil -based MRFs.

Table 1. An overview of performance indicators of rheological properties of diverse surfactants in MRFs

Diverse types of surfactants	Performance criteria (PC)			Gaps in knowledge	Remarks	Refs.
	Shear stress (SS)	Yield strength (YS)	Others PC assessed			
CIP	√	×	×	Few spectrums of CIP adopted. YS neglected	Higher distribution chain obtained from the mathematical models developed compared to conventional models	[16]
Particle size distributions of iron particles	√	×	×	Other PC and SS were not investigated	SS of mixed sized particles observed to be better than those of SS larger and smaller sized	[17]
Liquid carrier and micro-sized iron particles	×	Static yield stress investigated	×	Absence of YS studied.	Efficacy of scaling correlation for predicting YS established	[18]
cement paste modified with nanosilica	√	√		The SS, YS, and thermal properties of the surfactant's hybrid cannot handle that of CIP	The nonlinear parameters of the model are capable of determing the nano-silica on the rheological properties and compressive strength of cement	[19]
Particle chains	×	√	×	Non-appearance of YS studied.	Structure-enhanced of MFS is beneficial for the improvement of electrorheological fluids.	[20]

2. Materials and Methods

2.1. Materials and Reagents

The materials used for this project are magnetic particles (Carbonyl Iron particles/CIP of size range 3-5 um, obtained via Aliexpress from Chengdu Huarui Industrial Co. Ltd, China), carrier fluid (Paraffin oil obtained with a viscosity of 32 mPa, density of 0.8 g/cm^3 at room temperature, obtained from O and J Chemical Store, Delta State), and additive (Lithium grease, type: Filtex, obtained locally). The materials used for this project are magnetic particles (Carbonyl Iron particles /CIP) with a size range of 3-5 um, obtained via Aliexpress from Chengdu Huarui Industrial Co. Ltd, China. The carrier fluid used is paraffin oil with a viscosity of 32 mPa and a density of 0.8 g/cm^3 at room temperature, obtained from O and J Chemical Store in Delta State. The additive used is lithium grease of type Filtex, obtained locally. The equipment used for this project includes measuring cylinders, beakers, conical flask, rubber bowl, spatula, mixer, locally developed electromagnet [21], gaussmeter, filter paper, funnel, beam balance, mechanical stirrer, rheometer, and viscometer.

2.2. Synthesis of CIP Paraffin Oil Based MRFs

Sixteen samples of MRF were prepared following the standard procedure, which involves measuring the right proportion of each constituent needed, mixing appropriately, and using as suitable. The samples were prepared based on the Taguchi experimental design, and deployed the proportion of each constituent as discussed in [12]. For the project, the weight of CIP, paraffin oil, and lithium grease needed to arrive at the desired sample were measured using a beam balance. Then the measured CIP was mixed alongside the measured grease and agitated for 10 minutes at 2000 rpm using a mechanical stirrer and poured into a beaker containing the paraffin oil. They were further stirred at 2000 rpm using the mechanical stirrer for five (5) minutes. After stirring appropriately, a different portion was assessed for rheological responses: viscosity and shear stress, for the varied magnetic field. Details of the MRF production and its characterization are presented in the literature [12].

2.3. Setup for Rheological Testing

The observed viscosity for the different samples was measured using a viscometer. The applied magnetic field was induced in the sample using a locally developed magnetic device [21].

The schematics of the circuit diagram and components of the electro-magnet are shown in **Figure 1** and **Table 2**, respectively. Viscosity values were measured and recorded for different shearing speeds, sample compositions, and magnetic field capacities. Experimental data were also obtained for shear stress affected by shear strain with the aid of a rheometer.

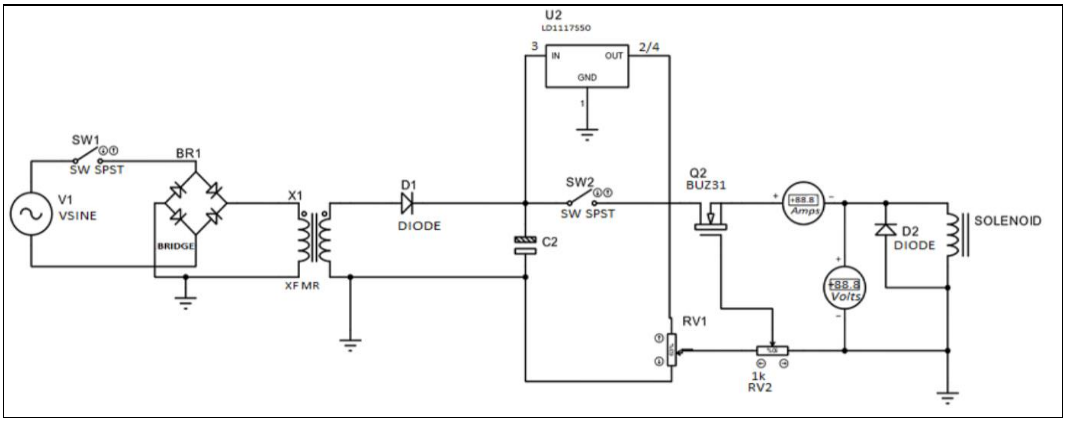

Figure 1. Circuit diagram of the solenoid driver [21]

Table 2. The different parts of the solenoid driver

S/No	Components	Specification	Quantity
1	Full wave bridge rectifier	IN4007 Diodes	4
2	Step down transformer	12V (1.5A)	2
3	Smoothing capacitor	2200uF (25V)	4
4	PN Diode		1
5	N-channel MOSFET		1
6	Potentiometer	10K Ohms	2
7	Voltage regulator	5V	1
8	Voltmeter/Ammeter	DS-288VC	1
9	Copper wire	1mm	12 yards

2.4. Rheological Modelling

The acquired experimental data were modelled using three well known and two lesser-known rheological equations: the Bingham Model, Herschel– Bulkley Model, Casson Model, Cross models, and Power Law [22]. These models are represented in Eqs. 1 to 5. The goal was to fit the experimental data to the model, determine the model parameters and yield stress, and then use the model to predict shear stresses in relation to the experimental data. The non-linear programming solver in Excel 2013 was utilised to determine the optimum model parameters. The Bingham model shown in Eq. (1) is the simplest and most utilised rheological model that has been applied in the modelling of MRFs [5], [23], [24]. Another model adopted for this work is the Herschel-Bulkley Model (Eq. 2), which is also widely applied in the modelling and simulation of MRFs [24], [25]. The Casson model (Eq. 3) has recorded some recent applications in the field of MRFs [25], hence its applicability is also investigated in this study. Two unpopular equations also investigated in this study are the Cross model (Eq. 4) and the power law (Eq. 5). These models, along with other rheological models, can be found in the review article [2], [22].

$$\tau = \tau_y + \mu\dot{\gamma} \tag{1}$$

$$\tau = \tau_y + \mu\dot{\gamma}^n \tag{2}$$

$$\sqrt{\tau} = \sqrt{\tau_y} + \sqrt{\mu\dot{\gamma}} \tag{3}$$

$$\tau = \tau_y[1 - \exp(-m\dot{\gamma})] + \mu\dot{\gamma}^n \tag{4}$$

$$\tau = K\dot{\gamma}^n \tag{5}$$

2.5. Analysis of Variance

The variance between the experimental data set and the predicted values using the divergent rheological models was analyzed using the ANOVA solver in Microsoft Excel version 2013. The p-values were calculated at a 5 % confidence level to ascertain significant variations in the data set of predicted shear stresses against the experimental values.

2.6. Error Computation

The error between predicted values using each model and experimental data was computed using Eqs. 6 – 9. The analysis of variance between the predicted shear stress and the experimental values was also calculated. The MATLAB code (2019 version) was developed to calculate the different error coefficients. Eqs. (6-9) were adopted to compute R-values, least-square error, mean square error, and mean absolute error, respectively.

$$R = \left(\frac{\sum_{i=1}^{n} \left(Y_{p.m} - Y_p\right)\left(Y_{e.m} - Y_e\right)}{\sum_{i=1}^{n} \left(Y_{p.m} - Y_p\right)^2 . \sum_{i=1}^{n} \left(Y_{e.m} - Y_e\right)^2} \right) \tag{6}$$

$$R^2 = 1 - \frac{\sum_{i-1}^{n} \left(Y_p - Y_e\right)^2}{\sum_{i-1}^{n} \left(Y_p - Y_{e.m}\right)^2} \tag{7}$$

$$\text{MSE}= \sqrt{\frac{\sum_{i=1}^{n} (Y_e - Y_p)^2}{n}} \tag{8}$$

$$\text{MAE} = \sum_{i=1}^{n} \frac{(Y_e - Y_p)}{n} \tag{9}$$

3. Results and Discussion

3.1. Equations and Their Parameters

Five different equations were used to model the rheological properties related to experiments conducted with the developed MRF. The parameters of these equations were evaluated using the multi-objective non-linear programming optimisation solver in Excel. The five models adopted are derived from various equations, namely the Bingham, Herschel–Bulkley, Casson, Cross models, and Power law.

3.1.1. The Bingham Model

The Bingham equation, which is a widely and commonly applied rheological model due to its simplicity and accuracy for low shear rates, was introduced for rheological data for shear stress (τ_s) values as affected by yield stress (τ_y), dynamic viscosity (μ), and shear rate ($\dot{\gamma}$). The equation with the optimum yield stress value obtained using the optimisation solver is shown in Eq. (10).

$$\tau_s = 531.76 + \mu\dot{\gamma} \tag{10}$$

3.1.2. The Herschel–Bulkley Model

The Herschel-Bulkley equation is another good equation for modelling MRF rheological behaviour, especially at high shear rates. The experimental data for this developed model were employed to fit the Herschel-Bulkley model and then optimised to arrive at the best-fit parameters, which are the yield stress (τ_y) and the Bulkley index (n). The new equation for predicting shear stress for varied dynamic viscosity and shear rate is given in Eq. (11).

$$\tau_s = 528.55 + \mu\dot{\gamma}^{1.01} \tag{11}$$

3.1.3. The Casson Model

The Casson model was developed to address the majority of problems associated with the Bingham model and Herschel-Bulkley model. There are different forms of this model, but the model by Saraswathamma et al. [25] was adopted for this study. It was used to fit the values from experimental data and determine the optimum yield stress for the model as written in Eq. (12).

$$\sqrt{63.36} = \sqrt{\tau_y} + \sqrt{\mu\dot{\gamma}^2} \tag{12}$$

3.1.4. The Cross Models

There are different cross models. The cross models are an improvement on the Herschel-Bulkley model to enhance its efficiency for modelling shear stresses at low value of shear rates. All parameters for the model were arrived at as shown in Eq. (13).

$$\tau = 491[1 - \exp(-0 * \dot{\gamma})] + \mu\dot{\gamma}^{1.09} \tag{13}$$

3.1.5. The Power Law

The power law has also been effectively applied for predicting shear stresses. Although its major weakness is its neglect of the yield stress, it was further studied in this research, and the parameter, which is its constant, K value was determined as shown in Eq. (14).

$$\tau_s = 442\,\mu\dot{\gamma}^n \tag{14}$$

4. Experimental Results

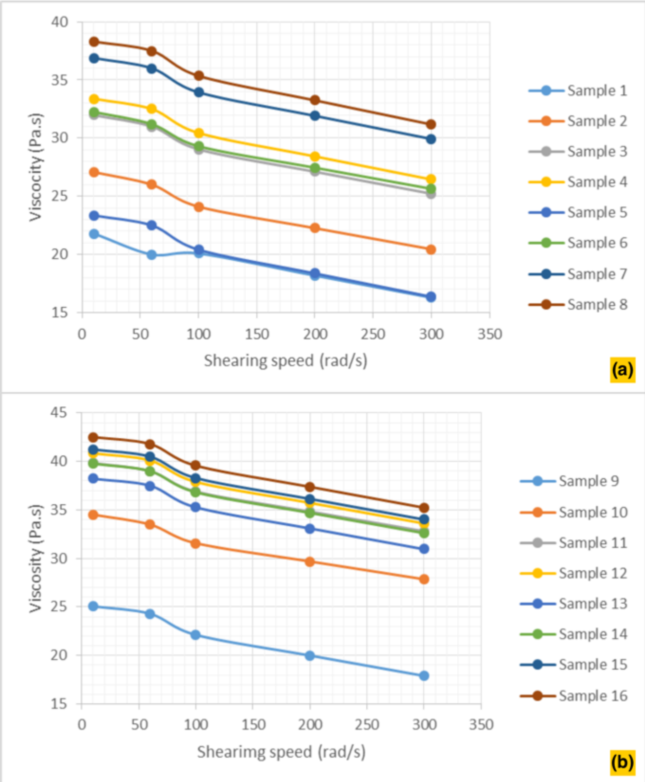

Figure 2. Viscosity versus shearing speed for a magnetic field strength of 1T: (a) samples 1-8 and (b) samples 9-16

Figure 2a and Figure 2b depict the relationship between viscosity and shearing speed for samples 1-8 and samples 9-16, for a fixed strength of 1T, respectively. As observed, values of varying capacity in the magnetic field and trends are consistent across all cases as well as the composition of each sample is detailed elsewhere [26]. Viscosity was measured and values were recorded for various shearing speeds ranging from 10 to 300 rad/s. A linear decrease in viscosity was observed for all samples as shearing speed increased, with sample 16 having the highest viscosity and sample 1 the lowest The decrease in viscosity with shearing speed, attributed to shear thinning at higher shearing rates aligns with findings in other studies [27]. The maximum viscosity was observed for sample 16 at the lowest shearing state.

Figure 3a and Figure 3b depict shear stress against shearing speed for samples 1-8 and samples 9-16, respectively. As observed, shear stress increased exponentially with shearing speed for all samples, with sample 5 having a maximum value of about 500 Pa and sample 16 having its maximum shear stress just below 3000 Pa. Values of shear stress are generally known to increase alongside shear rate for MRF, as reported several times in the literature [28]. The highest shear stress observed is recorded in sample 16 at the highest shearing speed.

Figure 4 shows how shear stress relates to shear rate using various chosen models for sample 11. Sample 11 was chosen because it had optimum parameters, as reported in another investigation.

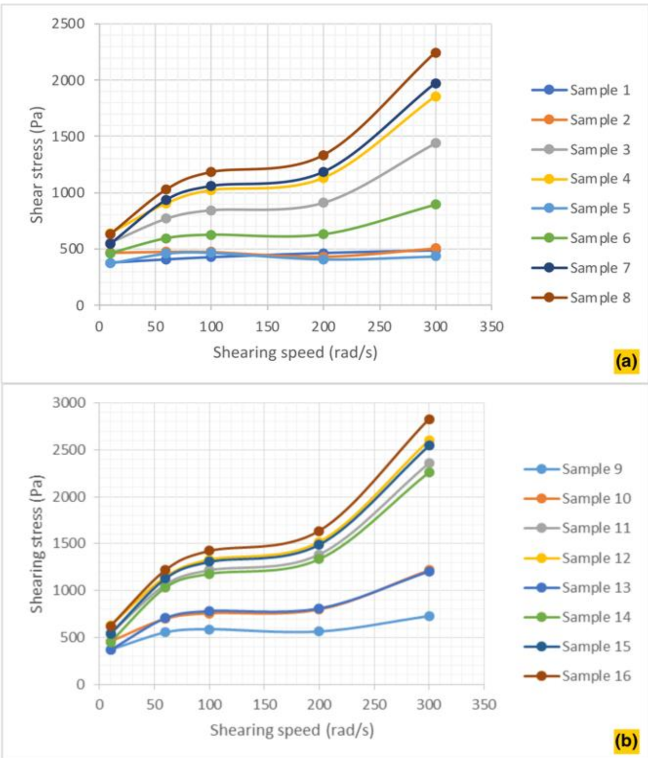

Figure 3. Shear stress versus shearing speed for a magnetic field strength of 1T: (a) samples 1-8 and (b) samples 9-16

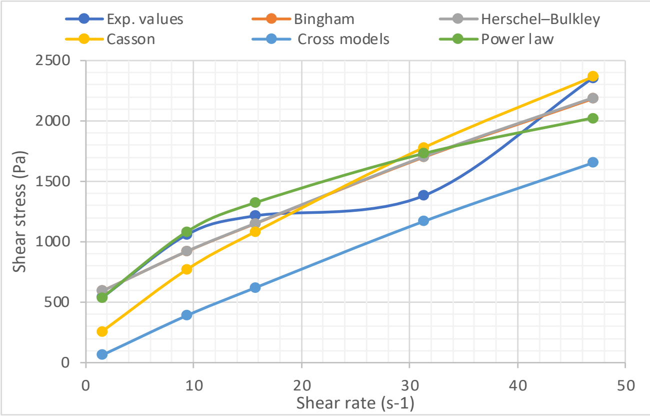

Figure 4. Shear stress versus shear rate for eleven samples based on different models

Overall, all models showed increasing shear stress values alongside shear rate, just like the experimental data set. However, the change was linear for cthe Cross model and Casson model, exponential for Bingham model, Herschel-Buclkley model, and power law model, but quadratic for the experimental values.

4.1. Analysis of Variance

The results obtained from the analysis of variance are shown in **Table 3**. The analysis included 5 rows representing the predicted shear stress values of the different models, as well as 4 rows showing the shear stress values obtained for the four different samples. The p-values for both rows and columns are well below 0.05, indicating a significant difference in shear stress values obtained using different models. Additionally, there is a significant variation in shear stress values recorded for the different samples tested.

Different values of errors computed using different error coefficients are tabulated in **Table 4**. As highlighted in the table of calculated errors, the R and R square values for the chosen models are very close to unity, with the Herschel-Bucklkey model having the highest R and R square values of 0.985815 and 0.984506, respectively, while the Casson model had the lowest R and R square values of 0.980626 and 0.967654, respectively.

Table 3. ANOVA Table for the shear stress values

Source of Variation	SS	Df	MS	F	P-value	F crit
Rows	10343486	4	2585871	149.5563	1.34E-14	2.866081
Columns	1170547	5	234109.4	13.53994	7.62E-06	2.71089
Error	345805.7	20	17290.28			
Total	11859839	29				

Table 4. Table of calculated errors

Error type	Bingham Model	Herschel–Bulkley Model	Casson Model	Cross models	Power law
R	0.98581	0.985815	0.980626	0.967709	0.978872
R_square	0.984477	0.984506	0.967654	0.658919	0.976235
MSE	177.4266	177.4041	260.8948	560.5749	220.5214
MAE	0.00018	0.001984	61.11409	531.7556	-28.0269
SEP	0.135017	0.135	0.198534	0.426583	0.167811
ADD	-1.49314	-1.38353	12.32435	48.94768	-4.25962

4.2. Estimated Yield Stress

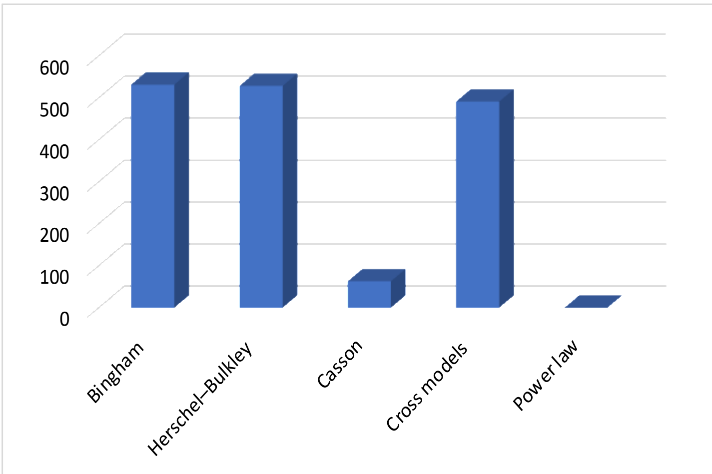

Figure 5. Graph of Yield stress vs the different models

The yield stress values for the different chosen models are presented in **Figure 5**. It is observed that the Bingham and Herschel-Bulkley models appeared with the highest predicted yield stress, while the Casson model had the lowest yield stress. It is worth noting that the values of predicted yield stress do not differ much for the Bingham model, Herschel-Bulkley model, and Cross model.

5. Variation of Different Modelling Techniques for Newly Developed MRFs

For the newly developed MRF, viscosity values were found to increase with the sample tags, indicating that as more portions of the CIPs and grease were mixed into prepared samples, the viscosities also increased. This correlates with previous findings [11], as viscosity was reported to increase with the addition of grease, thereby reducing the sedimentation ratio. Additionally, increasing viscosity values with added CIP is because CIP becomes solid dispersants in the prepared MRF. The linear decrease in viscosity with increasing shearing speed has been reported by several other studies [29], [30]. That is to say, if shearing is done at lower speeds, resistance is higher than when shearing is done at high shearing speeds. The maximum value of viscosity of 45 Pa.s was observed for the sample with the highest value of CIP (70% CIP by mass) and grease (3% by mass).

Shear stress for the investigated MRF increased with shearing speed due to shear thinning that may occur, as observed in several other studies. The implication is that the higher the value of shearing speed, the higher the shearing resistance. Also, shear stress values increased with the added proportion of CIP and grease. The maximum value of this developed MRF being about 2800 Pa compares favourably with conventional MRFs [31]. Predicted values of shear stresses were in close range to those of experimental values for Bingham, Herschel-Bulkley, power-law, and Casson models. However, the cross model gave wildly variant results from experimental values.

Significant variation was observed among the different modelling techniques; therefore, it is crucial to investigate which technique is most suitable for modelling MRFs. Information is scarce in the literature regarding the statistical comparison of modelling techniques. The results obtained from the Bingham model and Herschel-Bulkley model were very similar. However, the Herschel - Bulkley model provided the best result, as indicated by the calculated R-values. Several previous studies have demonstrated the effective prediction of shear stress values using the Bingham and Herschel-Bulkley techniques [28].

Yield values were predicted after using the non-linear programming Microsoft Excel solver to derive suitable parameters. The predicted yield stress values using the different models for the developed MRF were similar for the Bingham model, Herschel-Bulkley, and Cross models, whereas Casson's model gave a deviated value. This was likely because Casson's model was suitably developed for specific MRF types.

6. Conclusion

This work has studied commonly used rheological models for emerging MRFs, investigating the behaviour of some mostly used rheological models for application to predict shear stress and yield strength in novel MRF where Carbonyl-iron particles (CIP), low viscosity paraffin oil, and Lithium grease were used as the magnetic particles, carrier fluid, and additives, respectively. The obtained values of viscosity and shear stress were measured using a viscometer and Rheometer, respectively. There is a significant variation in the predicted results of every model. Overall, all the models gave relatively acceptable results. However, the Herschel-Bulkley model gave the best results, while the Casson model gave the worst results, judging by their values of errors. Itis concluded that, for CIP and Paraffin oil-based MRF, the Herschel-Bulkley model should be used for predicting its rheological characteristics

It is notably recorded that for this work, samples of a CIP, paraffin oil-based MRF enhanced with grease were developed, and their rheological properties assessed experimentally. A percentage of various rheological models was deployed to fit the data and predict the novel MRF's shear stresses and yield strength. Itis concluded that:

Outcomes of the experimental test indicates that the various rheological properties of the novel MRF were similar to those already reported in previous studies. The errors between predicted outcomes and the experimental values were within acceptable limits for all the models used to simulate the outcomes of experiments. All models gave results that differed significantly from experimental values. The recorded yield stress values given by the models: Bingham, Cross, and Herschel-Bulkley were similar.

Recommendations

Other optimisation methods for obtaining model parameters should be explored and compared for improved results. Alternative non-conventional modelling techniques should be investigated for predicting rheological properties of this novel MRF. Different rheological models should be tested on other MRFs to determine if similar discrepancies can be observed.

Authors' Declaration

Authors' contributions and responsibilities - The authors made substantial contributions to the conception and design of the study. The authors took responsibility for data analysis, interpretation, and discussion of results. The authors read and approved the final manuscript.

Funding – The research did not receive funding from any organization.

Availability of data and materials - All data is available from the authors.

Competing interests - The authors declare no competing interest.

Additional information – No additional information from the authors.

Nomenclature

m	: Casson coefficient	$\tau_{e.m}$	: Mean of experimental yield stress
Y_e	: Experimental yield stress	MSE	: Mean square error
Y_p	: Predicted yield	N	: Number of samples
$Y_{e.m}$	: Mean of experimental yield values	K	: Power law constatnt
$Y_{p.m}$	: Mean of predicted yield values	τ_p	: Predicted yield stress
n	: Hercschel-Bulkley exponent	$\dot{\gamma}$	: Shear rate
R^2	: Least square error	τ_s	: Shear stress
MAE	: Mean absolute error	μ	: Viscosity
$\tau_{p.m}$	: Mean of all predicted yield stress	τ_y	: Yield stress

References

[1] B. C. Kim, J. H. Chung, M. W. Cho, S. J. Ha, and G.-S. Yoon, "Magnetorheological fluid polishing using an electromagnet with straight pole-piece for improving material removal rate," *Journal of Mechanical Science and Technology*, vol. 32, no. 7, pp. 3345–3350, Jul. 2018, doi: 10.1007/s12206-018-0637-3.

[2] R. Ahamed, S.-B. Choi, and M. M. Ferdaus, "A state of art on magneto-rheological materials and their potential applications," *Journal of Intelligent Material Systems and Structures*, vol. 29, no. 10, pp. 2051–2095, Jun. 2018, doi: 10.1177/1045389X18754350.

[3] S. Zareie and A. Zabihollah, "The Recent Advances in Magnetorheological Fluids-Based Applications," in *Emerging Trends in Mechatronics*, IntechOpen, 2020. doi: 10.5772/intechopen.86178.

[4] M. Jackel, J. Kloepfer, M. Matthias, and B. Seipel, "The novel MRF-ball-clutch design – a MRF-safety-clutch for high torque applications," *Journal of Physics: Conference Series*, vol. 412, p. 012051, Feb. 2013, doi: 10.1088/1742-6596/412/1/012051.

[5] J. S. Kumar, P. S. Paul, G. Raghunathan, and D. G. Alex, "A review of challenges and solutions in the preparation and use of magnetorheological fluids," *International Journal of Mechanical and Materials Engineering*, vol. 14, no. 1, p. 13, Dec. 2019, doi: 10.1186/s40712-019-0109-2.

[6] E. Emagbetere and E. Zuokumor, "Artificial Neural Network for Modelling the Performance of Carbonyl-Iron Particle-Paraffin Oil-Based Magneto-Rheological Fluid," *Nigerian Research Journal of Engineering and Environmental Sciences*, vol. 7, no. 1, pp. 156–167, 2022, doi: 10.5281/zenodo.6722564.

[7] L. Vékás, D. Bica, I. Potencz, D. Gheorghe, O. Bãlãu, and M. Raça, "Concentration and composition dependence of rheological and magnetorheological properties of some magnetic fluids," in *Adsorption and Nanostructure*, Berlin, Heidelberg: Springer Berlin Heidelberg, pp. 104–109. doi: 10.1007/3-540-45405-5_19.

[8] R. Y. Hong, Z. Q. Ren, Y. P. Han, H. Z. Li, Y. Zheng, and J. Ding, "Rheological properties of water-based Fe3O4 ferrofluids," *Chemical Engineering Science*, vol. 62, no. 21, pp. 5912–5924, Nov. 2007, doi: 10.1016/j.ces.2007.06.010.

[9] Y. Rabbani, N. Hajinajaf, and O. Tavakoli, "An experimental study on stability and rheological properties of magnetorheological fluid using iron nanoparticle core–shell structured by

cellulose," *Journal of Thermal Analysis and Calorimetry*, vol. 135, no. 3, pp. 1687–1697, Feb. 2019, doi: 10.1007/s10973-018-7538-7.

[10] J. Liu, X. Wang, X. Tang, R. Hong, Y. Wang, and W. Feng, "Preparation and characterization of carbonyl iron/strontium hexaferrite magnetorheological fluids," *Particuology*, vol. 22, pp. 134–144, Oct. 2015, doi: 10.1016/j.partic.2014.04.021.

[11] M. Ashtiani, S. H. Hashemabadi, and A. Ghaffari, "A review on the magnetorheological fluid preparation and stabilization," *Journal of Magnetism and Magnetic Materials*, vol. 374, pp. 716–730, Jan. 2015, doi: 10.1016/j.jmmm.2014.09.020.

[12] E. Emagbetere, A. O. Egorerhua, J. O. Oyekale, and C. I. Ajuwa, "Taguchi and RSM in the Development of Cip-Parrafin-Oil Based Magneto-Rheological Fluid Enhanced with Grease," *NIPES - Journal of Science and Technology Research*, vol. 4, no. 2, 2022, doi: 10.37933/nipes/4.2.2022.6.

[13] A. Kaide, M. Kanda, H. Tochigi, and T. Saeki, "Preparation of Magnetorheological Fluid Using Stabilizing Additives," *MATEC Web of Conferences*, vol. 333, p. 02005, Jan. 2021, doi: 10.1051/matecconf/202133302005.

[14] Y.-Q. Guo, C.-L. Sun, Z.-D. Xu, and X. Jing, "Preparation and Tests of MR Fluids With CI Particles Coated With MWNTs," *Frontiers in Materials*, vol. 5, Aug. 2018, doi: 10.3389/fmats.2018.00050.

[15] L. Vékás, D. Bica, and M. V. Avdeev, "Magnetic nanoparticles and concentrated magnetic nanofluids: Synthesis, properties and some applications," *China Particuology*, vol. 5, no. 1–2, pp. 43–49, Feb. 2007, doi: 10.1016/j.cpart.2007.01.015.

[16] H. Khajehsaeid, N. Alaghehband, and P. K. Bavil, "On the Yield Stress of Magnetorheological Fluids," *Chemical Engineering Science*, vol. 256, p. 117699, Jul. 2022, doi: 10.1016/j.ces.2022.117699.

[17] C. Sarkar and H. Hirani, "Effect of Particle Size on Shear Stress of Magnetorheological Fluids," *Smart Science*, vol. 3, no. 2, pp. 65–73, Jan. 2015, doi: 10.1080/23080477.2015.11665638.

[18] Y. Yang, L. Li, and G. Chen, "Static yield stress of ferrofluid-based magnetorheological fluids," *Rheologica Acta*, vol. 48, no. 4, pp. 457–466, May 2009, doi: 10.1007/s00397-009-0346-z.

[19] A. Mohammed *et al.*, "Microstructure characterizations, thermal properties, yield stress, plastic viscosity and compression strength of cement paste modified with nanosilica," *Journal of Materials Research and Technology*, vol. 9, no. 5, pp. 10941–10956, Sep. 2020, doi: 10.1016/j.jmrt.2020.07.083.

[20] X. Tang, X. Zhang, R. Tao, and Y. Rong, "Structure-enhanced yield stress of magnetorheological fluids," *Journal of Applied Physics*, vol. 87, no. 5, pp. 2634–2638, Mar. 2000, doi: 10.1063/1.372229.

[21] E. Emagbetere *et al.*, "Development and modelling of an electro-magnet for magneto-rheological fluid experimental studies," in *3rd Borobudur International Symposium*, 2023, p. 020006. doi: 10.1063/5.0120840.

[22] A. Ghaffari, S. H. Hashemabadi, and M. Ashtiani, "A review on the simulation and modelling of magnetorheological fluids," *Journal of Intelligent Material Systems and Structures*, vol. 26, no. 8, pp. 881–904, May 2015, doi: 10.1177/1045389X14546650.

[23] E. Esmaeilnezhad, S. H. Hajiabadi, and H. J. Choi, "Effect of medium viscosity on rheological characteristics of magnetite-based magnetorheological fluids," *Journal of Industrial and Engineering Chemistry*, vol. 80, pp. 197–204, Dec. 2019, doi: 10.1016/j.jiec.2019.07.049.

[24] D. H. Bae, W. J. Han, C. Y. Gao, Y. Z. Dong, and H. J. Choi, "Preparation and Magnetorheological Response of Triangular-Shaped Single-Crystalline Magnetite Particle-Based Magnetic Fluid," *IEEE Transactions on Magnetics*, vol. 54, no. 11, pp. 1–4, Nov. 2018, doi: 10.1109/TMAG.2018.2832166.

[25] K. Saraswathamma, S. Jha, and P. Venkateswara Rao, "Rheological behaviour of Magnetorheological polishing fluid for Si polishing," *Materials Today: Proceedings*, vol. 4, no. 2, pp. 1478–1491, 2017, doi: 10.1016/j.matpr.2017.01.170.

[26] S. O. Ogundele, "Rheological Modelling of CIO paraffin oil based magneto-rheological fluids," 2022.

[27] A. B. Muddebihal and S. F. Patil, "Preparation and Study of Characteristics of Iron Based MR Fluids," *Materials Today: Proceedings*, vol. 24, pp. 1132–1137, 2020, doi:

10.1016/j.matpr.2020.04.426.

[28] B. S. Chen, J. Bin Jiang, and F. J. Zhang, "Studying on the Magnetorheological Fluids and its Rheometer," *Advanced Materials Research*, vol. 230–232, pp. 1396–1401, May 2011, doi: 10.4028/www.scientific.net/AMR.230-232.1396.

[29] M. Chand, A. Shankar, N. Ali, K. Jain, and R. P. Pant, "An improved properties of bidispersed magneto-rheological fluids," *RSC Adv.*, vol. 4, pp. 53960–53966, Sep. 2014, doi: 10.1039/C4RA07431A.

[30] M. A. Portillo and G. R. Iglesias, "Magnetic Nanoparticles as a Redispersing Additive in Magnetorheological Fluid," *Journal of Nanomaterials*, vol. 2017, pp. 1–8, 2017, doi: 10.1155/2017/9026219.

[31] F. D. Goncalves, M. Ahmadian, and J. D. Carlson, "The behaviour of magnetorheological fluids at high velocities and high shear rates," in *Electrorheological Fluids and Magnetorheological Suspensions (ERMR 2004)*, Jun. 2005, pp. 412–418. doi: 10.1142/9789812702197_0061.